

Accepted Manuscript

Title: Abatement of the fluorinated antidepressant fluoxetine (Prozac) and its reaction by-products by electrochemical advanced methods

Author: Claudio Salazar Carlota Ridruejo Enric Brillas Jorge Yáñez Héctor D. Mansilla Ignasi Sirés



PII: S0926-3373(16)30789-5
DOI: <http://dx.doi.org/doi:10.1016/j.apcatb.2016.10.026>
Reference: APCATB 15120

To appear in: *Applied Catalysis B: Environmental*

Received date: 5-8-2016
Revised date: 23-9-2016
Accepted date: 8-10-2016

Please cite this article as: Claudio Salazar, Carlota Ridruejo, Enric Brillas, Jorge Yáñez, Héctor D. Mansilla, Ignasi Sirés, Abatement of the fluorinated antidepressant fluoxetine (Prozac) and its reaction by-products by electrochemical advanced methods, *Applied Catalysis B, Environmental* <http://dx.doi.org/10.1016/j.apcatb.2016.10.026>

This is a PDF file of an unedited manuscript that has been accepted for publication. As a service to our customers we are providing this early version of the manuscript. The manuscript will undergo copyediting, typesetting, and review of the resulting proof before it is published in its final form. Please note that during the production process errors may be discovered which could affect the content, and all legal disclaimers that apply to the journal pertain.

Abatement of the fluorinated antidepressant fluoxetine (Prozac) and its reaction by-products by electrochemical advanced methods

Claudio Salazar^a, Carlota Ridruejo^b, Enric Brillas^{b,**}, Jorge Yáñez^a, Héctor D. Mansilla^a, Ignasi Sirés^{b,*}

^a *Facultad de Ciencias Químicas, Laboratorio de Trazas Elementales y Especiación (LabTres) Universidad de Concepción, Concepción, Chile. 4070371 Edmundo Larenas 129, Concepción, Chile*

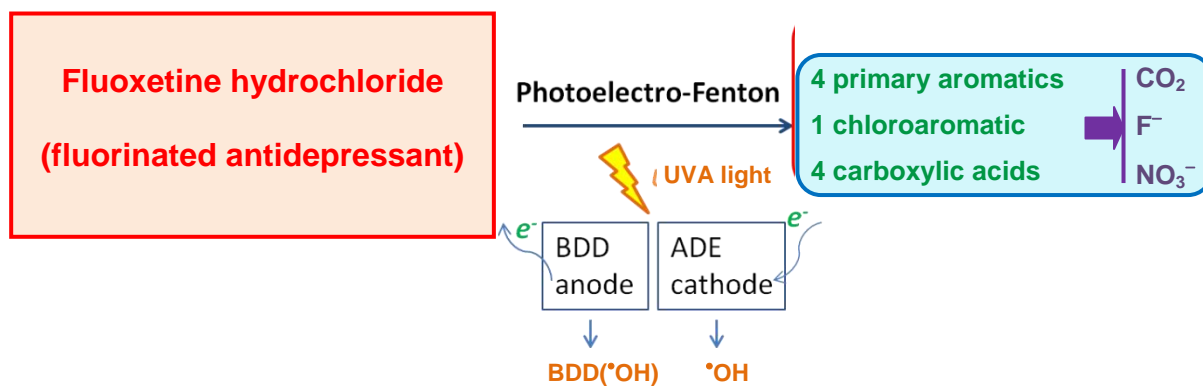
^b *Laboratori d'Electroquímica dels Materials i del Medi Ambient, Departament de Química Física, Facultat de Química, Universitat de Barcelona, Martí i Franquès 1-11, 08028 Barcelona, Spain*

* Corresponding author: Tel.: +34 934039240, Fax: +34 934021231

E-mail address: i.sires@ub.edu (I. Sirés)

**E-mail address: brillas@ub.edu (E. Brillas)

GRAPHICAL ABSTRACT



Research Highlights

- Fluoxetine hydrochloride treated with Pt, RuO₂-based or BDD anode and H₂O₂ generation
- Faster mineralization by PEF with a BDD anode due to BDD([•]OH), [•]OH and UVA light
- Pseudo-first-order decay by AO-H₂O₂, EF and, more rapidly, by PEF using a BDD anode
- Degradation of fluoxetine with F⁻ and NO₃⁻ formation and partial Cl⁻ oxidation to HClO
- Detection of 4 primary aromatics, 1 chloroaromatic derivative and 4 carboxylic acids

Abstract

The degradation of the fluorinated antidepressant fluoxetine, as hydrochloride, was comparatively studied in sulfate medium at pH 3.0 by anodic oxidation with electrogenerated H_2O_2 (AO- H_2O_2), electro-Fenton (EF) and photoelectro-Fenton (PEF). Experiments were performed with 100 mL solutions in an undivided tank reactor equipped with a Pt, RuO_2 -based or boron-doped diamond (BDD) anode and an air-diffusion cathode for continuous H_2O_2 production. The BDD anode showed higher mineralization rate due to the great production of physisorbed BDD($\bullet\text{OH}$), which has larger reactivity to oxidize the drug and intermediates. The degradation rate was enhanced by EF with 0.50 mM Fe^{2+} due to the additional production of $\bullet\text{OH}$ in the bulk from Fenton's reaction. The degradation was even faster using PEF owing to the additional photolytic action of UVA radiation. The most effective process was PEF with a BDD anode achieving 94% mineralization at 300 min. The fluoxetine decay followed a pseudo-first-order kinetics, being quicker in the order: AO- H_2O_2 < EF < PEF. The effect of the current density and drug concentration on the mineralization rate and fluoxetine decay was clarified. Oxidation of fluoxetine by hydroxyl radicals yielded four aromatic by-products, as found by GC-MS. Additionally, a chloroaromatic compound was identified as a result of the reaction of active chlorine, which was formed in situ from the oxidation of chloride ion at the BDD anode. Four short-chain linear carboxylic acids, being oxalic and formic acid more abundant, were identified. In PEF, fluorine atoms of fluoxetine were completely released as fluoride ion, whereas the initial nitrogen was converted to nitrate ion in all cases. A reaction pathway for fluoxetine mineralization by the electrochemical advanced methods is finally proposed.

Keywords: Anodic oxidation with electrogenerated H_2O_2 ; Electro-Fenton; Fluoxetine; Oxidation products; Photoelectro-Fenton

1. Introduction

Fluoxetine (see physicochemical characteristics in Table 1), also known by the trade names, Prozac, Sarafem or Fontex, is a fluorinated antidepressant belonging to the selective serotonin reuptake inhibitor (SSRI) class [1]. It is prescribed for the treatment of a number of mental disorders, such as depressive disorder, obsessive-compulsive disorder, bulimia nervosa, panic disorder and premenstrual dysphoric disorder. It is cited within the World Health Organization's List of Essential Medicines and considered as an important medication for a basic health system. The large production and prescription of fluoxetine in the entire world has caused its emerging occurrence in the aquatic environment, mainly in rivers at ng L^{-1} levels [2]. The presence of fluoxetine in the environment is due to its direct disposal from households, the excretion of unmetabolized drug and through pharmaceutical wastes. Its inefficient removal by common physicochemical and biological methods used in wastewater treatment plants (WWTPs) is a matter of concern [3,4]. Fluoxetine concentrations up to $0.01 \mu\text{g L}^{-1}$ have been determined in WWTP effluents and up to $4.7 \text{ mg (kg of organic carbon)}^{-1}$ has been found in sludges [1]. Furthermore, it has also been detected in drinking water at very low concentrations [1,5], which verifies the inefficiency of conventional treatments. Despite the low concentration of fluoxetine in the aquatic environment, several studies have revealed its bioaccumulation in fish tissues (from 0.14 to $1.02 \mu\text{g kg}^{-1}$) [6,7] and its toxicity over algae and small invertebrates [8-11]. In particular, this drug interacts with growth and reproduction processes in invertebrates [9]. This suggests that fluoxetine can exert potential noxious effects on living beings. Hence, new treatments for removing this pollutant and its metabolites from wastewater need to be devised. Recently, different methods such as sonolysis [12], advanced oxidation processes (AOPs) including $\text{O}_3/\text{H}_2\text{O}_2$ [13,14], TiO_2 photocatalysis in the presence of O_3 and H_2O_2 [13], and $\text{H}_2\text{O}_2/\text{UV}$ [15] have been reported within this framework. To the best of our knowledge, the degradation of fluoxetine using electrochemical AOPs (EAOPs) has not been yet reported in the literature.

Over the last 15 years, there has been an increasing interest in developing EAOPs based on in situ H_2O_2 production such as anodic oxidation with electrogenerated H_2O_2 (AO- H_2O_2), electro-Fenton (EF) and photoelectro-Fenton (PEF) [3,16-19]. These treatments involve the production of reactive oxygen species (ROS) on site, including H_2O_2 via two-electron reduction of O_2 gas (reaction (1)) at carbonaceous cathodes like BDD [20,21], activated carbon or graphite felt [22-25], carbon sponge [26], carbon nanotubes [27,28] and carbon-polytetrafluoroethylene (PTFE) gas diffusion devices [16,17,29,30].



In AO- H_2O_2 using an undivided electrolytic cell, dissolved organics can be oxidized by (i) direct charge transfer at the anode (M), (ii) reaction with physic/chemisorbed hydroxyl radical $\text{M}(\bullet\text{OH})$ originated from anodic water discharge, and (iii) reaction with H_2O_2 and its oxidation products like adsorbed hydroperoxyl radical $\text{M}(\text{HO}_2\bullet)$ produced at the anode as follows [3,18]:



The $\bullet\text{OH}$ radical is the second strongest oxidizing species known after fluorine. The high standard reduction potential of this radical ($E^\circ(\bullet\text{OH}/\text{H}_2\text{O}) = 2.80 \text{ V/SCE}$) explains its large ability to react with most of the organics, thus mineralizing them to carbon dioxide, water and inorganic ions [18,19]. The preferred anode in AO- H_2O_2 is the BDD thin-layer electrode due to its remarkable stability in acidic and alkaline conditions, low adsorption of organics and $\bullet\text{OH}$, and larger O_2 -evolution overvoltage as compared with conventional anodes like Pt and PbO_2 [31-34]. Due to these properties, great amounts of reactive BDD($\bullet\text{OH}$) are produced at the BDD anode from reaction (3), which enhances the degradation of organics [35,36].



In EF, the oxidation ability of electrogenerated H_2O_2 is upgraded by addition of Fe^{2+} , since it generates homogeneous $\bullet\text{OH}$ and Fe^{3+} ion via Fenton's reaction (4) at optimum pH ~ 3 [3,4,37]. Organics are mainly oxidized by both, adsorbed $\text{M}(\bullet\text{OH})$ and homogeneous $\bullet\text{OH}$. The effectiveness of reaction (4) is assured by its propagation from the cathodic reduction of Fe^{3+} to Fe^{2+} [22,34]. However, the degradation of aromatic compounds in EF is inhibited due to the formation of stable complexes between Fe(III) and short carboxylic acids [29,30]. To overcome this problem, UVA photoassisted PEF process, in which the solution is irradiated with artificial UVA light, has been successfully applied [29,38-41]. This radiation facilitates the mineralization of organics because the Fe^{2+} regeneration and $\bullet\text{OH}$ production in the bulk are enhanced upon photoreduction of $\text{Fe}(\text{OH})^{2+}$ species by reaction (5) and photolysis of Fe(III)-carboxylate complexes by reaction (6).



Lately, we have been interested in assessing the performance of EAOPs for the removal of organic pollutants (pesticides, dyes and pharmaceuticals) from wastewater in order to show their viability at larger scale. However, the scale-up is limited by the high cost of the BDD anode, thus being necessary to test the oxidation ability of these methods with much less expensive anode materials such as RuO_2 -based ones, routinely used in chloride media [3]. For this reason, we have undertaken a study on the abatement of fluoxetine by AO- H_2O_2 , EF and PEF using Pt, RuO_2 -based and BDD anodes. The classical Pt anode was chosen to clearly analyze the degradation power of the cheaper RuO_2 -based one, being both of them considered as low oxidation power anodes.

This paper reports the degradation behavior of fluoxetine by using its commercial form, i.e., hydrochloride salt. In order to clarify the oxidation pathways and compare the oxidation power of these processes with Pt, RuO_2 -based and BDD as anodes, higher drug contents as compared to those

found in the environment were used. The influence of current density (j) and drug content on the mineralization rate and drug decay was examined. The time course of fluoxetine concentration and the evolution of by-products such as inorganic ions, short-chain aliphatic acids and aromatic compounds were determined by chromatographic techniques. From these results, a plausible reaction pathway for fluoxetine mineralization by means of the EAOPs has been finally proposed.

2. Experimental

2.1. Chemicals

Fluoxetine hydrochloride (99% purity) was purchased from Fluka (St. Louis, MO, USA) and used as received. Maleic, fumaric, oxalic and formic acids were of analytical grade supplied by Sigma-Aldrich (St. Louis, MO, USA) and Panreac (Barcelona, Spain). Sodium sulfate and heptahydrated iron(II) sulfate were of analytical grade supplied by Fluka and Sigma-Aldrich, respectively. Ultrapure water from a Millipore Milli-Q system (Billerica, MA, USA) with resistivity $> 18 \text{ M}\Omega \text{ cm}$ at $25 \text{ }^\circ\text{C}$ was utilized to prepare all the solutions. The initial pH of solutions was adjusted to 3.0 with analytical grade sulfuric acid supplied by Merck (Darmstadt, Germany). Other chemicals were either of HPLC or analytical grade purchased from Merck and Panreac.

2.2. Instruments

The pH values of solutions were determined with a Crison GLP 22 pH-meter (Barcelona, Spain). Total organic carbon (TOC) was measured with a Shimadzu VCSN TOC analyzer (Kyoto, Japan), which was coupled with a Shimadzu TNM-1 unit to obtain the total nitrogen (TN) in the solution. Reproducibility of TOC measurements was $\pm 1\%$. Electrochemical assays were performed at constant j with an Amel 2053 potentiostat-galvanostat (Milano, Italy). The stability of the electrolytic system was monitored from the continuous measurement of the potential difference of the cell by using a Demestres 601BR digital multimeter (Barcelona, Spain). High-performance liquid chromatography (HPLC) measurements were carried out with a Waters 600 LC (Cerdanyola

del Vallès, Spain) coupled with a Waters 996 photodiode array detector. For reversed-phase HPLC, the LC was fitted with a Waters Spherisorb ODS2-C18 5 μ m, 150 mm \times 4.6 mm (i.d.), column at 25 °C and the detector was set at $\lambda = 227$ nm for quantification of fluoxetine. For ion-exclusion HPLC, a Bio-Rad Aminex HPX 87H, 300 mm \times 7.8 mm (i.d.), column at 35 °C was used, and the detector was set at $\lambda = 210$ nm for quantification of carboxylic acids. Inorganic anions were quantified by ion chromatography. F⁻ and Cl⁻ concentrations were determined using a Shimadzu 10 Avp LC fitted with a Shim-Pack IC-A1S, 100 mm \times 4.6 mm (i.d.), anion column at 40 °C coupled with a Shimadzu CDD 10 Avp conductivity detector. NO₃⁻ concentration was measured with a Kontron 465 LC (Bonaduz, GR, Switzerland) equipped with the above column at 35 °C and coupled with a Waters 432 conductivity detector and a Kontron 332 UV/Vis detector set at $\lambda = 214$ nm. The NH₄⁺ content was determined with an Alpkem Flow Solution IV flow injection system (Hood River, OR, USA) through colorimetric analysis based on the standard indophenol blue reaction. Gas chromatography-mass spectrometry (GC-MS) analysis was made with an Agilent Technologies 6890N GC (Tokyo, Japan) fitted with a non-polar Teknokroma Sapiens-X5ms 0.25 μ m, 30 m \times 0.25 mm (i.d.), column and coupled with a 5975C MS operating in EI mode at 70 eV.

2.3. Electrolytic system

Fluoxetine hydrochloride solutions were electrolyzed using an undivided, open glass tank reactor of 150 mL with a double jacket for circulation of thermostated water at 35 °C, under vigorous stirring at 800 rpm provided by a magnetic PTFE follower. The anode was either a Pt sheet of 99.99% purity supplied by SEMPSA (Barcelona, Spain), a DSA-Cl₂ (RuO₂-based anode) plate purchased from NMT Electrodes (Pinetown, South Africa) or a BDD thin-film electrode supplied by NeoCoat (La-Chaux-de-Fonds, Switzerland). The cathode was a carbon-PTFE air-diffusion electrode (ADE) provided by E-TEK (Somerset, NJ, USA), mounted as described elsewhere [17] and fed with air pumped at 1 L min⁻¹ for continuous H₂O₂ generation. The geometric area of all the electrodes was 3 cm² and the interelectrode gap was kept at about 1 cm. In PEF trials,

the solution was irradiated with a 6-W Philips black light blue tube lamp placed 7 cm above its surface. The lamp emitted in the λ range of 320-400 nm ($\lambda_{\max} = 360$ nm) and supplied 5 W m^{-2} , as detected with a Kipp&Zonen CUV 5 UV radiometer (Delft, The Netherlands). Before use, the BDD anode and ADE cathode were polarized in 0.050 M Na_2SO_4 at $j = 100 \text{ mA cm}^{-2}$ for 180 min to remove the impurities from the anode surface and to activate the cathode.

2.4. Analytical methods

For TOC measurements, all the samples withdrawn from solutions were filtered with $0.45 \mu\text{m}$ PTFE membrane filters from Whatman (Madrid, Spain). From these data, the mineralization current efficiency (MCE) at a given current I (in A) and electrolysis time t (in h) was calculated from equation (7) [42]:

$$\% \text{ MCE} = \frac{n F V_s \Delta(\text{TOC})_{\text{exp}}}{4.32 \times 10^7 m I t} \times 100 \quad (7)$$

where F is the Faraday constant ($96,487 \text{ C mol}^{-1}$), V_s is the solution volume (in L), $\Delta(\text{TOC})_{\text{exp}}$ is the solution TOC abatement (in mg L^{-1}), 4.32×10^7 is a conversion factor to homogenize units ($3,600 \text{ s h}^{-1} \times 12,000 \text{ mg C mol}^{-1}$) and $m = 17$ is the number of carbon atoms of fluoxetine. The number n of electrons needed for the theoretical total mineralization of the protonated form of the drug was taken as 86 from equation (8), considering the formation of CO_2 and F^- and NO_3^- ions, as will be discussed below.



During the EF and PEF treatments, a small volume of acetonitrile was added to the samples collected before chromatographic analysis in order to stop the degradation of fluoxetine and its by-products. All the HPLC and ion chromatography measurements were made by injecting 20-25 μL aliquots into the LC systems. The mobile phase for reversed-phase HPLC was a 50% (v/v) acetonitrile/water (10 mM KH_2PO_4 , pH 3.0) mixture at 1 mL min^{-1} and chromatograms displayed a

peak for fluoxetine at retention time (t_r) of 12.3 min. For ion-exclusion HPLC, the mobile phase was 4 mM H_2SO_4 at 0.6 mL min^{-1} and chromatograms exhibited peaks related to oxalic acid ($t_r = 6.8$ min), maleic acid ($t_r = 8.1$ min), formic acid ($t_r = 13.7$ min) and fumaric acid ($t_r = 15.2$ min). For F^- and Cl^- determination, a solution with 2.4 mM tris(hydroxymethyl)aminomethane and 2.5 mM phthalic acid at pH 4.0 was eluted at 1.5 mL min^{-1} as mobile phase, whereas for determining NO_3^- , the mobile phase was prepared with boric acid, sodium gluconate, sodium tetraborate, acetonitrile, butanol and glycerine, being eluted at 2.0 mL min^{-1} .

TOC and kinetic measurements under each experimental condition were done in triplicate with good reproducibility and average values are given throughout the text. In figures, error bars related to the 95% confidence interval of each average data are also depicted.

The stable aromatic by-products formed during the electrolysis of 100 mL of a 0.490 mM fluoxetine hydrochloride solution after 15, 120 and 240 min of AO- H_2O_2 at $j = 100$ mA cm^{-2} were analyzed by GC-MS using a NIST05-MS library for identification. After each electrolysis, the organic components were extracted out with CH_2Cl_2 (3×15 mL) and the organic volume was reduced to ca. 1 mL after drying over anhydrous Na_2SO_4 followed by filtration. The temperature program for GC-MS analysis was 36 °C for 1 min, 5 °C min^{-1} up to 320 °C and hold time 10 min. The temperature of the inlet, source and transfer line was 250, 230 and 300 °C, respectively.

3. Results and discussion

3.1. Degradation of fluoxetine by AO- H_2O_2 with different anodes

To check the oxidation ability of adsorbed $\text{M}(\bullet\text{OH})$ and generated H_2O_2 as well as of weaker ROS like $\text{HO}_2\bullet$ produced in AO- H_2O_2 from reactions (1)-(3), 100 mL of solutions containing 0.490 mM fluoxetine hydrochloride and 0.050 M Na_2SO_4 as background electrolyte at pH 3.0 were comparatively treated by this EAOP using either Pt, RuO_2 -based or BDD as the anode at $j = 100$ mA cm^{-2} for 360 min. The solution pH did not change significantly over a time. However, at the

end of the process, pH was slightly more acidic ($\text{pH} \approx 2.7\text{-}2.8$), which is probably due to the formation of products like aliphatic carboxylic acids [3,18,41].

Fig. 1a depicts the time course of normalized TOC for the three trials. TOC content was reduced by 18% and 32% after 360 min using Pt and RuO_2 anodes, which indicates the poor mineralization ability of these electrodes. This observation implies that $\text{Pt}(\bullet\text{OH})$ and, to a lesser extent, H_2O_2 have low ability to oxidize fluoxetine and its degradation intermediates. The higher oxidation power of the RuO_2 anode can then be accounted for by a greater activity of physisorbed hydroxyl radical. In contrast, BDD anode exhibits 77% TOC abatement after 360 min, which agrees with its larger oxidation ability. The physisorbed nature of $\text{BDD}(\bullet\text{OH})$, along with their formation at larger anodic potentials, entails a much higher oxidation efficiency for the AO- H_2O_2 treatment of fluoxetine.

Since j determines the quantity of oxidizing species in AO- H_2O_2 , the effect of this operation parameter on the mineralization of the above 0.490 mM fluoxetine hydrochloride solution was examined in the range 33.3-150 mA cm^{-2} using the BDD anode. As can be seen in Fig. 1b, an increase in j caused a quicker TOC decay, reaching final abatements of 51%, 66%, 77% and 87% for growing j values. This behavior can be simply associated with the increasing generation rate of reactive $\text{BDD}(\bullet\text{OH})$ according to reaction (3). Nevertheless, the percentage of TOC removed was not proportional to the applied j , which suggests the occurrence of parasitic reactions that diminished the oxidation ability of the process. This behavior can be confirmed from the corresponding MCE values calculated from Eq. (7) and presented in Fig. 1c. The current efficiency underwent a gradual decay with increasing j , attaining final values of 9.6%, 6.2%, 4.3% and 3.6%, respectively, after 360 min. This decay in MCE is typical of EAOPs and can be explained by the acceleration of parasitic reactions of $\text{BDD}(\bullet\text{OH})$, thus being less available to oxidize organic molecules. The most important among those reactions is the oxidation of $\text{BDD}(\bullet\text{OH})$ to O_2 gas via reaction (9) [35,36]. Moreover, the dimerization of this radical leads to H_2O_2 by reaction (10),

which can in turn react with the radical by reaction (11) [3,18,34,38]. The production of other weaker oxidants at the BDD anode like the peroxodisulfate ion ($S_2O_8^{2-}$) from the oxidation of SO_4^{2-} via reaction (12) and ozone via reaction (13) can also reduce the BDD(\bullet OH) content and hence, the oxidation power of the AO- H_2O_2 process [18,35,36].



The progressive reduction of MCE at long time observed in all curves of Fig. 1c is also noticeable. This tendency can be associated with the gradual loss of organic load along with the production of more refractory by-products [18,36].

3.2. EF and PEF treatment of fluoxetine with different anodes

The EF process of the above 0.490 mM fluoxetine hydrochloride solution at pH 3.0 was studied with a BDD anode at 100 mA cm^{-2} by adding either 0.50 or 1.00 mM Fe^{2+} as catalyst of Fenton's reaction (4). Fig. 2a shows a fast TOC decay for both assays, obtaining 86% and 91% TOC reduction, respectively. The quicker mineralization for 1.00 mM Fe^{2+} can be explained by the greater generation of \bullet OH in the bulk from the concomitant acceleration of Fenton's reaction (4). Comparing with the AO- H_2O_2 process, the superiority of both EF assays is explained by the production of \bullet OH in the bulk, which acts in concomitance with physisorbed BDD(\bullet OH). For example, after 120 min of electrolysis, TOC was reduced by 42% in AO- H_2O_2 (see Fig. 1a) and to a much larger extent of 53% and 70% for EF with 0.50 and 1.00 mM Fe^{2+} , respectively (see Fig. 2a).

Analogous PEF trials were comparatively performed employing a 6 W UVA lamp to irradiate the solutions. Fig. 2a depicts a similar mineralization rate at both Fe^{2+} concentrations, at least from 120 min, reaching 93% of TOC reduction at 360 min. PEF performed better than EF due to the synergistic action of BDD($\bullet\text{OH}$), $\bullet\text{OH}$ and UVA radiation over fluoxetine and its by-products. It is noteworthy that UVA light caused a 90% of TOC decay in only 180 min, which is greater than 70% achieved in EF process with 1.00 mM Fe^{2+} (see Fig. 2a).

All the aforementioned findings indicate that BDD is the best anode and the oxidation power of the EAOPs increased in the sequence: AO- H_2O_2 < EF < PEF. Since similar mineralization rates were found for the PEF treatment with 0.50 and 1.00 mM Fe^{2+} , the former content was chosen for addressing the effect of different experimental variables like j , anode material and drug concentration on the performance of this EAOP, as will be discussed below.

Fig. 2a shows the progressive rise in TOC abatement when j increased from 33.3 to 100 mA cm^{-2} for the PEF degradation of 0.490 mM fluoxetine hydrochloride solutions with 0.50 mM Fe^{2+} . This trend can be ascribed to the greater production rate of BDD($\bullet\text{OH}$) and H_2O_2 due to the acceleration of reactions (3) and (1), respectively, along with the subsequent higher generation rate of $\bullet\text{OH}$ from Fenton's reaction (4), thereby yielding larger amounts of photoactive species that tended to be more rapidly degraded upon exposure to UVA irradiation. Nevertheless, similar TOC removals of 90%, 92% and 93% were finally obtained at 33.3, 66.6 and 100 mA cm^{-2} , respectively.

The inset panel of Fig. 2a depicts a drop in MCE for the above trials as j was increased. Apart from reactions (9)-(13) that mainly cause a loss of BDD($\bullet\text{OH}$), other parasitic reactions can lead to a fall of $\bullet\text{OH}$ content in the bulk. These include its dimerization by reaction (14) and its destruction by Fe^{2+} and H_2O_2 via reactions (15) and (16), respectively [3,18,38-42]. Maximum current efficiencies of 35.6% at 33.3 mA cm^{-2} , 26.0% at 66.7 mA cm^{-2} and 20.3% at 100 mA cm^{-2} were obtained, finally decaying to 17.0%, 8.7% and 5.8%. The drop of MCE over time can be again

related to the loss of organic matter and the production of more stable molecules that are hardly destroyed by BDD(\bullet OH), \bullet OH and UVA light, thus impeding the total mineralization by PEF.



Fig. 2b illustrates the comparative normalized TOC abatement for a 0.490 mM fluoxetine hydrochloride solution with 0.50 mM Fe^{2+} treated by PEF using either a Pt, RuO_2 -based or BDD anode at $j = 100 \text{ mA cm}^{-2}$. Compared with the analogous curves for AO- H_2O_2 (without Fe^{2+}) of Fig. 1a, the PEF processes exhibited higher mineralization. The influence of the anode was very relevant again, which suggests a significant influence of the adsorbed M(\bullet OH) on the degradation process. Fig. 2b shows that the mineralization rate increased in the order: RuO_2 -based \leq Pt \ll BDD. While for the two former anodes about 80% of TOC was removed after 360 min of electrolysis, a higher TOC reduction of 93% TOC was achieved with BDD. Taking into account the poor mineralization achieved with Pt and RuO_2 -based anodes in AO- H_2O_2 (see Fig. 1a), it can be inferred that \bullet OH and UVA radiation were the main oxidants in PEF with those anodes. In contrast, the quicker and larger mineralization attained with BDD suggests a more significant role of physisorbed BDD(\bullet OH) for oxidizing the by-products, decisively contributing to the action of \bullet OH and UVA light.

The effect of initial drug concentration on the performance of PEF process with a BDD anode was studied using 0.50 mM Fe^{2+} at 100 mA cm^{-2} . Fig. 3 corroborates the large effectiveness of this EAOP for removing the TOC from all the solutions, reaching $> 88\%$ of mineralization. Although progressively better percentages of TOC removal (up to 94%) were obtained in the 0.245-0.835 mM range, further diminishing, an increasing amount of TOC was always abated at higher drug concentrations, thereby upgrading the efficiency of the process. This behavior is shown in the inset

panel of Fig. 3, where the MCE values for the above trials are presented. For example, after 60 min of electrolysis, the current efficiency raised gradually, attaining 11.0%, 20.0%, 26.0% and 29.8% for increasing drug contents. Since the same quantity of BDD(\bullet OH) and \bullet OH is expected to be accumulated at a constant j in the BDD/ADE cell, the greater efficiency results from the deceleration of parasitic reactions (9)-(16). This explanation is supported by the continuous drop in MCE with prolonging electrolysis, as can be seen for all the assays in the inset panel of Fig. 3, partly resulting from the gradually lower organic load.

From these results, it can be concluded that the best EAOP, namely PEF with a BDD anode, becomes more efficient at low j values and high drug concentrations, i.e., when parasitic reactions are strongly decelerated. This favors the reaction of organics with BDD(\bullet OH) and \bullet OH, yielding higher amounts of photoactive intermediates that can be quickly removed under UVA irradiation. Despite this, 93-94% TOC reduction was reached as maximum, therefore remaining a small proportion of highly persistent by-products in solution.

3.3. Decay kinetics of fluoxetine by EAOPs with a BDD anode

The kinetics for the removal of 0.490 mM fluoxetine under AO-H₂O₂, EF and PEF conditions using a BDD/ADE tank reactor at $j = 100 \text{ mA cm}^{-2}$ was followed by reversed-phase HPLC. A blank experiment demonstrated that the solution remained stable upon UVA irradiation in the absence of current (data not shown). This informs about the photostability of the drug, being BDD(\bullet OH) and/or \bullet OH the main oxidizing species generated in all the EAOPs tested.

Fig. 4 highlights the total removal of fluoxetine in all the treatments, needing decreasing times of 220 min in AO-H₂O₂, 120 min in EF and 50 min in PEF. This trend agrees with the relative oxidation power stated above for these EAOPs and confirms the low oxidation power of BDD(\bullet OH) in AO-H₂O₂ and the much quicker action of \bullet OH in the bulk in EF as well as in PEF, where its formation is largely induced by the photolytic reaction (5). Fig. 4 shows a good agreement with a pseudo-first-order reaction and the excellent linear correlations can be seen in the inset panel. The

apparent rate constants (k_1), i.e., the slopes of such straight lines, were $3.1 \times 10^{-4} \text{ s}^{-1}$ ($R^2 = 0.995$) in AO-H₂O₂, $5.7 \times 10^{-4} \text{ s}^{-1}$ ($R^2 = 0.996$) in EF and $1.10 \times 10^{-3} \text{ s}^{-1}$ ($R^2 = 0.987$) in PEF. These results suggest that fluoxetine reacts with a low and constant amount of BDD(\bullet OH) and/or \bullet OH in all cases as a result of the very short lifetime of the reactive radicals [18].

The influence of j and drug concentration on fluoxetine degradation kinetics was also assessed. As can be seen in Fig. 5a, an increase in j caused a faster removal of the drug for a 0.420 mM solution under PEF conditions with a BDD anode. Total disappearance was achieved after 100, 80 and 50 min at 33.3, 66.7 and 100 mA cm⁻², respectively. This occurs owing to the larger generation of BDD(\bullet OH) and \bullet OH with increasing j , as explained above. The inset panel of Fig. 5a depicts the straight lines obtained for these trials considering a pseudo-first-order reaction, yielding a k_1 value of $5.6 \times 10^{-4} \text{ s}^{-1}$ ($R^2 = 0.994$) at 33.3 mA cm⁻², $8.1 \times 10^{-4} \text{ s}^{-1}$ ($R^2 = 0.990$) at 66.7 mA cm⁻² and $1.10 \times 10^{-3} \text{ s}^{-1}$ ($R^2 = 0.987$) at 100 mA cm⁻². These data reveal a two-fold enhancement of k_1 upon a three-fold increase of j (from 33.3 to 100 mA cm⁻²), which confirms the concomitant loss of BDD(\bullet OH) and \bullet OH due to the acceleration of parasitic reactions (9)-(16). On the other hand, Fig. 5b shows the good performance of the PEF process with a BDD anode for complete removal of fluoxetine, requiring between 20 and 180 min at starting contents ranging from 0.263 to 0.925 mM. The inset panel of Fig. 5b shows the linear correlations found for a pseudo-first-order decay in all these trials, yielding decreasing k_1 values of $2.42 \times 10^{-3} \text{ s}^{-1}$ ($R^2 = 0.992$), $1.10 \times 10^{-3} \text{ s}^{-1}$ ($R^2 = 0.987$), $6.8 \times 10^{-4} \text{ s}^{-1}$ ($R^2 = 0.993$) and $3.8 \times 10^{-4} \text{ s}^{-1}$ ($R^2 = 0.995$) as the drug content rises. This behavior corroborates the complexity of the fluoxetine removal since it does not follow a real pseudo-first-order kinetics, whose intrinsic characteristic should be the absence of drug concentration effect on k_1 . It can be deduced that, at each fluoxetine content, different steady-state concentrations of BDD(\bullet OH) and \bullet OH are achieved, being highly dependent on their reaction with by-products and the extent of parasitic reactions.

3.4. Product identification: Aromatics, carboxylic acids and inorganic ions

Table 2 summarizes the characteristics of four aromatic by-products formed directly from fluoxetine (**1**) degradation and detected by GC-MS during the AO-H₂O₂ treatment of a 0.490 mM fluoxetine hydrochloride solution at pH 3.0 and 100 mA cm⁻². The aromatics identified were 4-trifluoromethylphenol (**2**), styrene (**3**), its derivative benzaldehyde (**4**) and a product arising from internal cyclization, 1-methyl-3,4-dihydro-2H-quinoline (**5**). Moreover, one chloroaromatic derivative like 4-chlorophenyl benzoate (**6**) was detected as well. This species may result from the attack of active chlorine (Cl₂/HClO) formed from the oxidation of Cl⁻ ion, which is present in the hydrochloride salt, at the BDD anode [43,44]. Note that the same intermediates are expected in EF and PEF because of the generation of the same kinds of oxidizing species in all the EAOPs.

Ion-exclusion chromatograms of the same solution, degraded by different treatments using a BDD/ADE cell at $j = 100 \text{ mA cm}^{-2}$, exhibited peaks associated to four final carboxylic acids, namely maleic (**7**), fumaric (**8**), oxalic (**9**) and formic (**10**). Under the conditions used in EF and PEF, most of these acids exist in solution in the form of Fe(III) complexes [18,24,34].

Fig. 6a-c illustrates the evolution of detected carboxylic acids in AO-H₂O₂, EF and PEF. Maleic and fumaric acid, formed from the cleavage of the benzene ring of aromatic by-products [3,18,29], were found in concentrations below 0.4 mg L⁻¹ in all cases, being at trace level in EF and completely disappearing at electrolysis times ≤ 360 min. This is indicative of a very rapid removal of both Fe(III)-maleate and Fe(III)-fumarate complexes by BDD([•]OH) and [•]OH. In contrast, oxalic acid and pre-eminently formic acid, formed from the oxidation of the two former acids and converted to CO₂ [38-42], were accumulated to a much larger extent. Maximum contents of 3.1 (300 min), 5.3 (240 min) and 6.5 (120 min) mg L⁻¹ of oxalic acid were determined in AO-H₂O₂, EF and PEF, respectively, which dropped to 1.6, 2.6 and 0.1 mg L⁻¹ after 360 min of electrolysis. This means that Fe(III)-oxalate species are oxidized by BDD([•]OH) and photolyzed by UVA light, as established in previous work [24,34,38-42]. Similarly, formic acid attained 18.2 (240 min), 18.8

(240 min) and 22.8 (180 min) mg L⁻¹ as maximal for such processes, decreasing up to a final value of 6.7 mg L⁻¹ in AO-H₂O₂ and disappearing completely in EF and more quickly in PEF. Therefore, Fe(III)-formate complexes are oxidized by BDD(•OH) and •OH, and can also be photodecomposed by UVA radiation. Considering these results and the resulting mass balance, it can be stated that the remaining carboxylic acids contribute in 2.1, 0.7 and < 0.1 mg L⁻¹ of TOC to the final solutions obtained by AO-H₂O₂, EF and PEF, which are negligible values compared to the corresponding 23, 14 and 7 mg L⁻¹ of TOC (see Fig. 1b, 2a and 2b). Hence, EAOPs generate unidentified by-products that are more persistent than short-chain linear carboxylic acids to degradation by •OH and UVA light.

The time course of inorganic ions detected during the above processes was also assessed. Fig. 7a highlights the continuous release of F (1.470 mM, 27.93 mg L⁻¹ in the solution) as F⁻ ion, as considered in reaction (8), meaning that organofluorinated by-products were slowly but gradually destroyed. At the end of AO-H₂O₂, EF and PEF degradation at $j = 100 \text{ mA cm}^{-2}$, F⁻ content accounted for 70.2%, 86.7% and 100% of initial F after 360 min, respectively. This agrees with the relative oxidation power of these treatments and confirms the total destruction of all fluorinated intermediates only under the synergistic action of BDD(•OH), •OH and UVA light in the powerful PEF. This result highlights the positive action of the radiation to decontaminate the fluoxetine hydrochloride solution. On the other hand, Fig. 7b reveals the continuous disappearance of Cl⁻ ion (0.490 mM, 17.30 mg L⁻¹ in the hydrochloride solution), reaching 80-86% removal after 360 min of all trials. It is well known that this ion can be oxidized to chlorine on BDD by reaction (17), being subsequently hydrolyzed to hypochlorous acid by reaction (18) [36,39,43,44]. The generated active chlorine mixture (Cl₂/HClO) possesses a strong oxidizing ability at pH 3.0, which can explain the formation of chloroderivative **6**.





The fate of the initial N (0.490 mM, 6.86 mg L⁻¹ in the solution) for the above assays was finally investigated. NO₃⁻ ions were always detected in the electrolyzed solutions, as written in the total mineralization equation (8), but neither NO₂⁻ nor NH₄⁺ ions were found. Fig. 8a shows the continuous accumulation of N-NO₃⁻ up to 1.81 mg L⁻¹ in AO-H₂O₂, 3.84 mg L⁻¹ in EF and 2.03 mg L⁻¹ in PEF after 360 min, corresponding to 26.3%, 56.0% and 29.6% of initial N. The TN content of all the solutions underwent a progressive drop over time, as can be seen in Fig. 8b. It was reduced by 13.0%, 43.8% and 47.4% in AO-H₂O₂, EF and PEF, respectively. The loss of TN mainly suggests the release of volatile nitrogen compounds, like N₂ and N_xO_y, as also reported for other *N*-aromatics [38-42]. Note that the final solutions of AO-H₂O₂ and PEF contained refractory nitrogenated by-products, probably aliphatic derivatives, but in the case of EF, only NO₃⁻ ions were present in the medium. This means that the [•]OH radicals formed in the bulk in the EF process are able to destroy all nitrogenated by-products, whereas the action of UVA light in PEF promotes the formation of quite persistent nitrogenated by-products (17.8% of initial N) that become accumulated in the final treated solution.

3.5. Proposed reaction sequence for fluoxetine mineralization

Based on the identified products, Fig. 9 presents a plausible reaction sequence for fluoxetine mineralization by EAOPs with a BDD anode. The main oxidants are the physisorbed BDD([•]OH) and/or [•]OH, although the degradation with active chlorine is also feasible, as stated above. In EF and PEF, final carboxylic acids are predominantly in the form of Fe(III) complexes, which has been only remarked for oxalic and formic acids for the sake of simplicity.

The degradation of the parent molecule **1** occurs via four parallel paths. The cleavage of one of the C-O bonds with simultaneous hydroxylation yields the fluorinated compound **2**. The rest of the fluoxetine molecule is then either transformed into compound **3** with loss of its lateral amino chain,

followed by oxidation to compound **4**, or undergo an internal cyclization via the amino group to yield the quinoline **5**. The chlorinated compound **6** can be formed from the loss of the lateral amino chain by oxidation with $\bullet\text{OH}$, in concomitance with chlorination of the benzoate moiety in C₄ position with release of the trifluoromethyl group. The gradual degradation of these aromatics and their intermediates leads to the generation of F⁻ and NO₃⁻ ions, along with the production of short-chain linear aliphatic acids **7-10**. Acids **7** and **8** are oxidized to acids **9** and **10**, which are slowly destroyed by BDD($\bullet\text{OH}$) in AO-H₂O₂, whereas their Fe(III) complexes can be removed by $\bullet\text{OH}$ in EF or photolyzed by UVA light in PEF with regeneration of Fe²⁺ (see reaction (6)).

4. Conclusions

The use of a BDD anode in the AO-H₂O₂, EF and PEF treatment of acidic fluoxetine hydrochloride solutions in sulfate medium yielded a much larger mineralization than that obtained with Pt and RuO₂-based ones, which emphasizes the great oxidation power of physisorbed BDD($\bullet\text{OH}$). The synergistic action of $\bullet\text{OH}$ in the bulk in EF enhanced the degradation process, being further upgraded by the photolytic action of UVA light in PEF. The latter process with a BDD anode was then the most effective one, leading to 94% of TOC reduction as maximal. Current efficiency rose at lower j and higher drug content. The fluoxetine decays obeyed a pseudo-first-order reaction, becoming faster in the order: AO-H₂O₂ < EF < PEF. The apparent rate constant increased with increasing j and with decreasing initial drug concentration. Four primary aromatic by-products coming from cleavage, hydroxylation, oxidation and internal cyclization steps, as well as one chloroaromatic derivative resulting from the action of active chlorine, were identified. Ion-exclusion HPLC allowed the identification of large quantities of oxalic and formic acids. They were slowly destroyed by BDD($\bullet\text{OH}$) in AO-H₂O₂, but their Fe(III) complexes were rapidly photolyzed by UVA light in PEF. F atoms were completely released as F⁻ ion only in PEF, where the initial N was partially mineralized as NO₃⁻ ion with a significant loss of volatile compounds.

Acknowledgments

The authors acknowledge financial support from project CTQ2013-48897-C2-1-R (MINECO, FEDER, EU). C. Salazar thanks FONDECYT Postdoctoral Grant 3150253 and CONICYT/FONDAP 15110019.

References

- [1] V. Calisto, V.I. Esteves, *Chemosphere* 77 (2009) 1257-1274.
- [2] J. Roberts, A. Kumar, J. Du, C. Hepplewhite, D.J. Ellis, A.G. Christy, S.G. Beavis, *Sci. Total Environ.* 541 (2016) 1625-1637.
- [3] I. Sirés, E. Brillas, *Environ. Int.* 40 (2012) 212-229.
- [4] P. Verlicchi, M. Al Aukidy, E. Zambello, *Sci. Total Environ.* 429 (2012) 123-155.
- [5] A. Izadyar, D.R. Arachchige, H. Cornwell, J.C. Hershberger, *Sens. Actuators B* 223 (2016) 226-233.
- [6] S. Chu, C.D. Metcalfe, *J. Chromatogr. A* 1163 (2007) 112-118.
- [7] G. Paterson, C.D. Metcalfe, *Chemosphere* 74 (2008) 125-130.
- [8] D.J. Johnson, H. Sanderson, R.A. Brain, C.J. Wilson, K.R. Solomon, *Ecotoxicol. Environ. Safe.* 67 (2007) 128-139.
- [9] A.R.R. Péry, M. Gust, B. Vollat, R. Mons, M. Ramil, G. Fink, T. Ternes, J. Garric, *Chemosphere* 73 (2008) 300-304.
- [10] M. Gust, T. Buronfosse, L. Giamberini, M. Ramil, R. Mons, J. Garric, *Environ. Pollut.* 157 (2009) 423-429.
- [11] C. Rivetti, B. Campos, C. Barata, *Aquat. Toxicol.* 170 (2016) 289-296.
- [12] E.A. Serna-Galvis, J. Silva-Agredo, A.L. Giraldo-Aguirre, R.A. Torres-Palma, *Sci. Total Environ.* 524-525 (2015) 354-360.

- [13] F. Méndez-Arriaga, T. Otsu, T. Oyama, J. Gimenez, S. Esplugas, H. Hidaka, N. Serpone, *Water Res.* 45 (2011) 2782-2794.
- [14] A. Aghaeinejad-Meybodi, A. Ebadi, S. Shafiei, A.R. Khataee, M. Rostampour, *J. Taiwan Chem. Eng.* 48 (2015) 40-48.
- [15] H.-W. Yu, T. Anumol, M. Park, I. Pepper, J. Scheideler, S.A. Snyder, *Water Res.* 81 (2015) 250-260.
- [16] I. Sirés, N. Oturan, M.A. Oturan, R.M. Rodríguez, J.A. Garrido, E. Brillas' *Electrochim. Acta* 52 (2007) 5493-5503.
- [17] M. Skoumal, C. Arias, P.L. Cabot, F. Centellas, J.A. Garrido, R.M. Rodríguez, E. Brillas, *Chemosphere* 71 (2008) 1718-1729.
- [18] I. Sirés, E. Brillas, M.A. Oturan, M.A. Rodrigo, M. Panizza, *Environ. Sci. Pollut. Res.* 21 (2014) 8336-8367.
- [19] S. Vasudevan, M.A. Oturan, *Environ. Chem. Lett.* 12 (2014) 97-108.
- [20] K. Cruz-González, O. Torres-López, A. García-León, J.L. Guzmán-Mar, L.H. Reyes, A. Hernández-Ramírez, J.M. Peralta-Hernández, *Chem. Eng. J.* 160 (2010) 199-206.
- [21] K. Cruz-González, O. Torres-López, A.M. García-León, E. Brillas, A. Hernández-Ramírez, J.M. Peralta-Hernández, *Desalination* 286 (2012) 63-68.
- [22] A. Özcan, M.A. Oturan, N. Oturan, Y. Şahin, *J. Hazard. Mater.* 163 (2009) 1213-1220.
- [23] M. Panizza, M.A. Oturan, *Electrochim. Acta* 56 (2011) 7084-7087.
- [24] A. El-Ghenymy, R.M. Rodríguez, E. Brillas, N. Oturan, M.A. Oturan, *Environ. Sci. Pollut. Res.* 21 (2014) 8368-8378.
- [25] F.E.F. Rêgo, A.M.S. Solano, I.C. da Costa Soares, D.R. da Silva, C.A. Martínez-Huitle, M. Panizza, *J. Environ. Chem. Eng.* 2 (2014) 875-880.
- [26] A. Özcan, Y. Sahin, A.S. Koparal, M.A. Oturan, *J. Electroanal. Chem.* 616 (2008) 71-78.
- [27] A.R. Khataee, M. Safarpour, A., Naseri, M. Zarei, *J. Electroanal. Chem.* 672 (2012) 53-62.

- [28] A. Khataee, A. Khataee, M. Fathinia, B. Vahid, S.W. Joo, *J. Ind. Eng. Chem.* 19 (2013) 1890-1894.
- [29] F.C. Moreira, S. Garcia-Segura, R.A.R. Boaventura, E. Brillas, V.J.P. Vilar, *Appl. Catal. B: Environ.* 160-161 (2014) 492-505.
- [30] A. Thiam, M. Zhou, E. Brillas, I. Sirés, *Appl. Catal. B: Environ.* 150-151 (2014) 116-125.
- [31] L. Liu, G. Zhao, M. Wu, Y. Lei, R. Geng, *J. Hazard. Mater.* 168 (2009) 179-186.
- [32] M. Hamza, R. Abdelhedi, E. Brillas, I. Sirés, *J. Electroanal. Chem.* 627 (2009) 41-50.
- [33] G. Zhao, Y. Zhang, Y. Lei, B. Lv, J. Gao, Y. Zhang, D. Li, *Environ. Sci. Technol.* 44 (2010) 1754-1759.
- [34] E.B. Cavalcanti, S. Garcia-Segura, F. Centellas, E. Brillas, *Water Res.* 47 (2013) 1803-1815.
- [35] B. Marselli, J. García-Gomez, P.A. Michaud, M.A. Rodrigo, C. Comninellis, *J. Electrochem. Soc.* 150 (2003) D79-D83.
- [36] M. Panizza, G. Cerisola, *Chem. Rev.* 109 (2009) 6541-6569.
- [37] Y. Wang, H. Zhao, G. Zhao, *Appl. Catal. B: Environ.* 164 (2015) 396-406.
- [38] X. Florenza, A.M.S. Solano, F. Centellas, C.A. Martínez-Huitle, E. Brillas, S. Garcia-Segura, *Electrochim. Acta* 142 (2014) 276-288.
- [39] A. Thiam, I. Sirés, J.A. Garrido, R.M. Rodríguez, E. Brillas, *Sep. Purif. Technol.* 140 (2015) 43-52.
- [40] Q. Peng, H. Zhao, L. Qian, Y. Wang, G. Zhao, *Appl. Catal. B: Environ.* 174-175 (2015) 157-166.
- [41] A. Thiam, E. Brillas, J.A. Garrido, R.M. Rodríguez, I. Sirés, *Appl. Catal. B: Environ.* 180 (2016) 227-236.
- [42] E.J. Ruiz, A. Hernández-Ramírez, J.M. Peralta-Hernández, C. Arias, E. Brillas, *Chem. Eng. J.* 171 (2011) 385-392.
- [43] J. De Laat, G.T. Le, B. Legube, *Chemosphere* 55 (2004) 715-723.

- [44] C. Salazar, I. Sirés, C.A. Zaror, E. Brillas, *Electrocatalysis* 4 (2013) 212-223.

Figure captions

Fig. 1. Normalized TOC decay vs. electrolysis time for the degradation of 100 mL of a 0.490 mM fluoxetine hydrochloride solution in 0.050 M Na₂SO₄ at pH 3.0 and 35 °C by anodic oxidation with electrogenerated H₂O₂ (AO-H₂O₂) using a stirred tank reactor equipped with an air-diffusion cathode (ADE) and electrodes of 3 cm² area. (a) Anode: (●) Pt, (◆) RuO₂-based and (▲) BDD at current density of 100 mA cm⁻². (b) BDD anode, current density: (●) 33.3 mA cm⁻², (■) 66.7 mA cm⁻², (▲) 100 mA cm⁻² and (◆) 150 mA cm⁻². (c) Variation of mineralization current efficiency with electrolysis time for the above assays.

Fig. 2. Change of normalized TOC removal with electrolysis time for the treatment of 100 mL of a 0.490 mM fluoxetine hydrochloride solution in 0.050 M Na₂SO₄ at pH 3.0 and 35 °C by electro-Fenton (EF) and photoelectro-Fenton (PEF) using the same cell of Fig. 1. (a) BDD anode; EF with (◆) 0.50 and (□) 1.00 mM Fe²⁺ at current density of 100 mA cm⁻²; PEF with 0.50 mM Fe²⁺ at current density: (▲) 33.3 mA cm⁻², (▼) 66.7 mA cm⁻² and (●) 100 mA cm⁻²; (■) PEF with 1.00 mM Fe²⁺ at current density of 100 mA cm⁻². The inset panel presents the corresponding variation of mineralization current efficiency. (b) PEF with 0.50 mM Fe²⁺ at current density of 100 mA cm⁻². Anode: (●) Pt, (◆) RuO₂-based and (▲) BDD.

Fig. 3. Effect of drug concentration on TOC abatement vs. electrolysis time for the degradation of 100 mL of fluoxetine hydrochloride solutions in 0.050 M Na₂SO₄ with 0.50 mM Fe²⁺ at pH 3.0 and 35 °C by PEF using a BDD/ADE tank reactor at current density of 100 mA cm⁻². Fluoxetine hydrochloride content: (■) 0.245 mM, (●) 0.490 mM, (◆) 0.835 mM and (▲) 1.225 mM. The corresponding mineralization current efficiency is depicted in the inset panel.

Fig. 4. Fluoxetine concentration decay for the treatment of 100 mL of 0.490 mM drug solutions in 0.050 M Na₂SO₄ at pH 3.0 and 35 °C with a BDD/ADE tank reactor at current density of 100 mA

cm^{-2} . (▲) AO- H_2O_2 , (■) EF with 0.50 mM Fe^{2+} and (●) PEF with 0.50 mM Fe^{2+} . The inset panel shows the kinetic analysis assuming a pseudo-first-order reaction for fluoxetine.

Fig. 5. Time course of fluoxetine concentration for the PEF degradation of 100 mL of drug solutions in 0.050 M Na_2SO_4 with 0.50 mM Fe^{2+} at pH 3.0 and 35 °C using a BDD/ADE cell. (a) 0.420 mM fluoxetine hydrochloride, current density: (▲) 33.3 mA cm^{-2} , (▼) 66.7 mA cm^{-2} and (●) 100 mA cm^{-2} . (b) Fluoxetine hydrochloride concentration: (■) 0.263 mM, (●) 0.420 mM, (◆) 0.647 mM and (▲) 0.925 mM at current density of 100 mA cm^{-2} . The kinetic analysis for a pseudo-first-order reaction is presented in the inset panels.

Fig. 6. Evolution of the concentration of: (□) maleic (7), (△) fumaric (8), (○) oxalic (9) and (◇) formic (10) acids detected during the treatment of 100 mL of a 0.490 mM fluoxetine hydrochloride solution in 0.050 M Na_2SO_4 at pH 3.0 and 35 °C using a BDD/ADE tank reactor at current density of 100 mA cm^{-2} . (a) AO- H_2O_2 , (b) EF with 0.50 mM Fe^{2+} and (c) PEF with 0.50 mM Fe^{2+} .

Fig. 7. Time-course of the concentration of (a) fluoride and (b) chloride ions during the (▲) AO- H_2O_2 , (○) EF with 0.50 mM Fe^{2+} and (●) PEF with 0.50 mM Fe^{2+} , under the conditions of Fig. 6.

Fig. 8. Evolution of (a) N-NO_3^- and (b) total nitrogen during the (▲) AO- H_2O_2 , (○) EF with 0.50 mM Fe^{2+} and (●) PEF with 0.50 mM Fe^{2+} processes under the conditions of Fig. 6.

Fig. 9. Proposed reaction sequence for the mineralization of fluoxetine by EAOPs using a BDD anode.

Table 1

Physicochemical characteristics of fluoxetine.

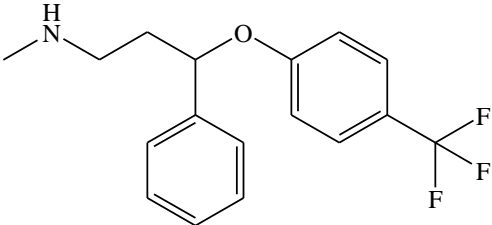
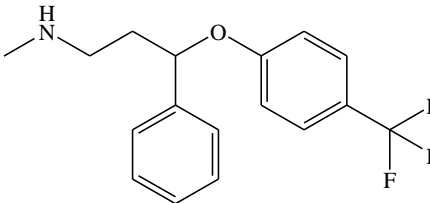
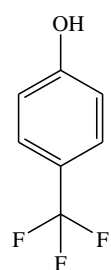
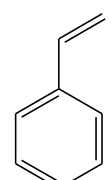
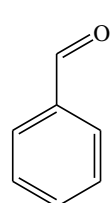
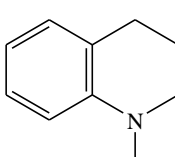
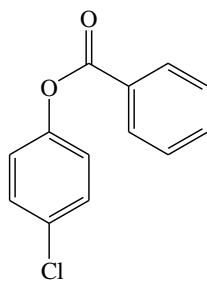
IUPAC name	<i>N</i> -methyl-3-phenyl-3-[4-(trifluoromethyl)phenoxy]propan-1-amine
Molecular structure	
Empirical formula	C ₁₇ H ₁₈ F ₃ NO
Molar mass	309.33 g mol ⁻¹
Melting point	179 to 182 °C
Boiling point	395 °C
Solubility in water	14 g L ⁻¹ (at 20 °C)

Table 2

Organic intermediates detected by GC-MS during the AO-H₂O₂ treatment of 100 mL of a 0.49 mM fluoxetine hydrochloride solution in 0.050 M Na₂SO₄ at pH 3.0 and 35 °C using a BDD/ADE cell at 100 mA cm⁻².

Number	Compound	Molecular structure	<i>t_r</i> ^a (min)	Main fragmentation ions (<i>m/z</i>)
1	Fluoxetine		33.3	309, 44
2	4-Trifluoromethylphenol		13.1	162, 143, 112
3	Styrene		7.4	104, 78, 51
4	Benzaldehyde		9.6	106, 77
5	1-Methyl-3,4-dihydro-2H-quinoline		20.6	147, 132, 118

6 4-Chlorophenyl benzoate

27.7

232, 105

^a Retention time

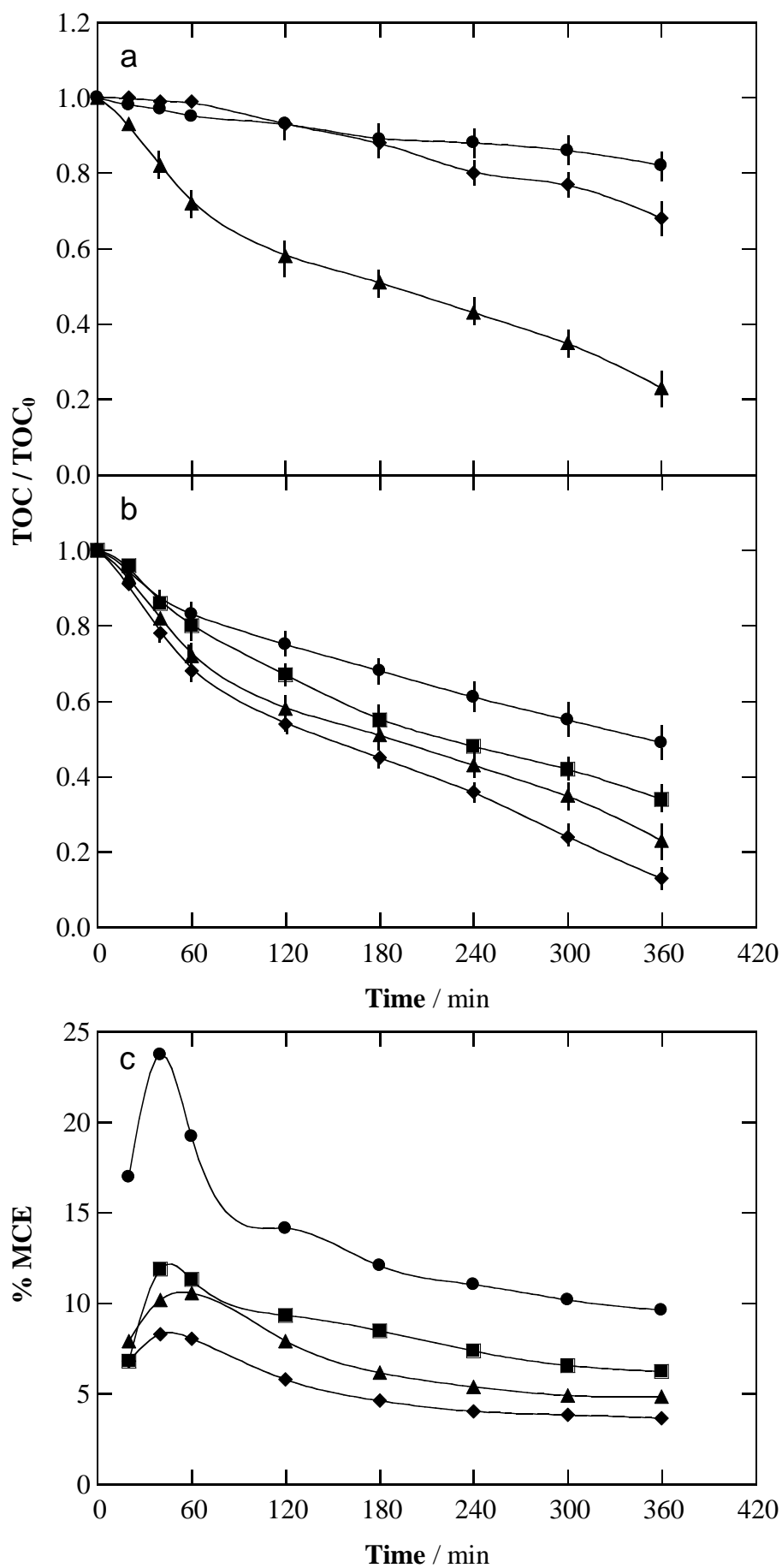


Fig. 1

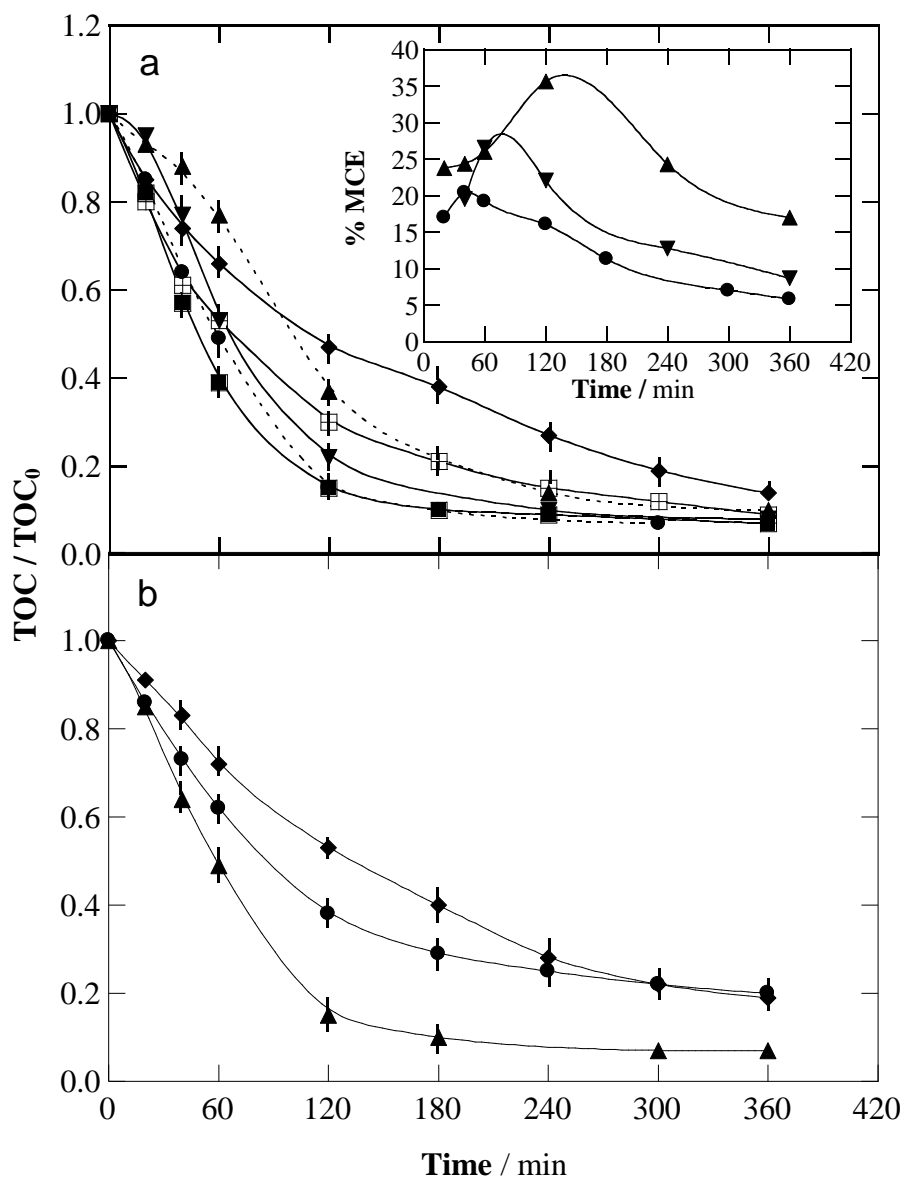
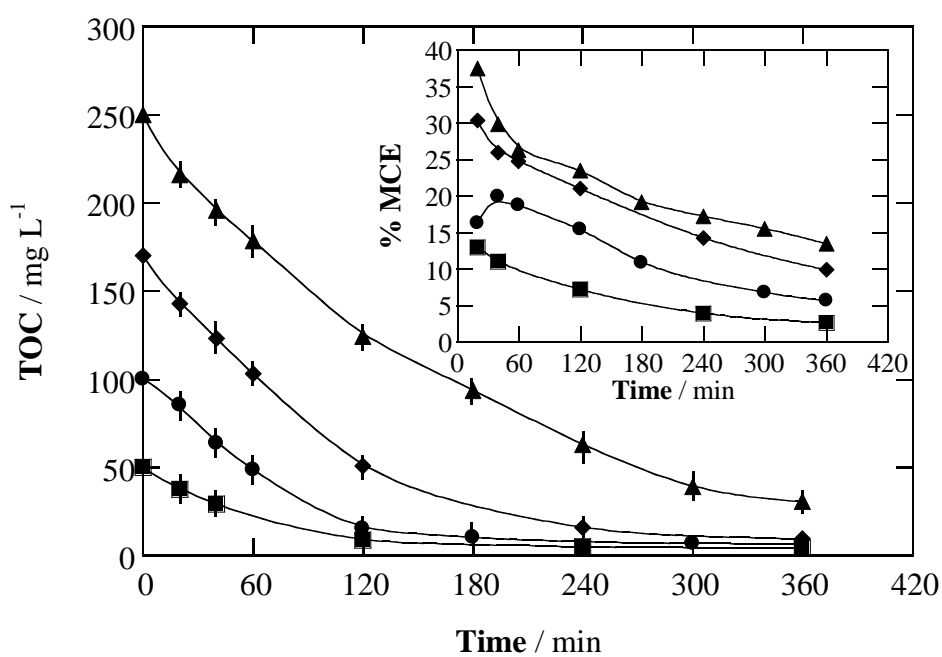


Fig. 2

**Fig. 3**

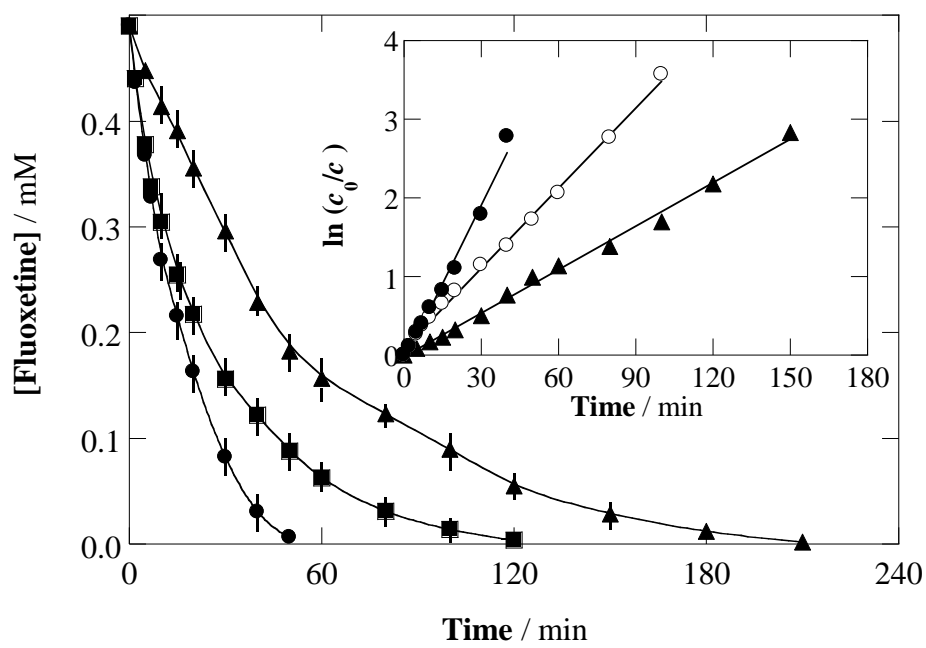


Fig. 4

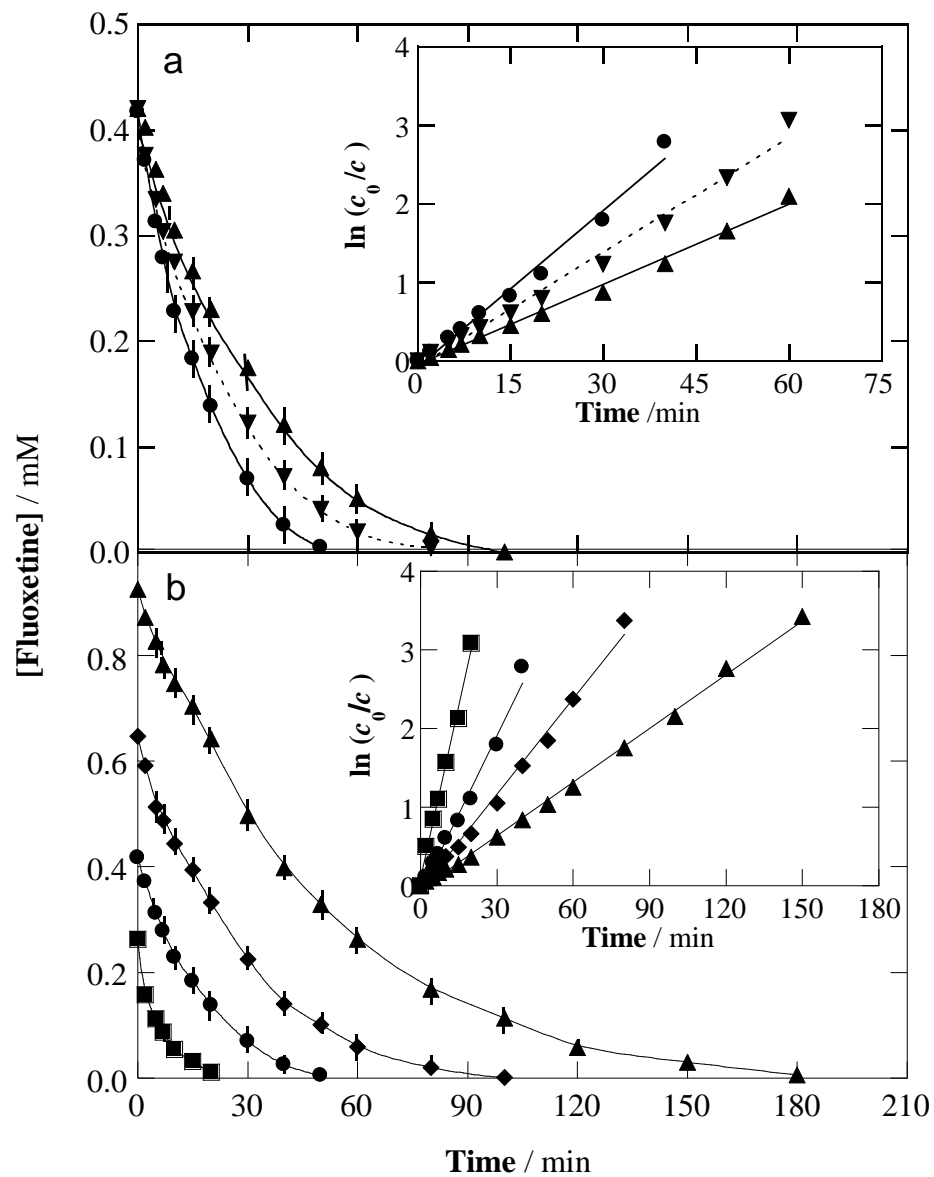


Fig. 5

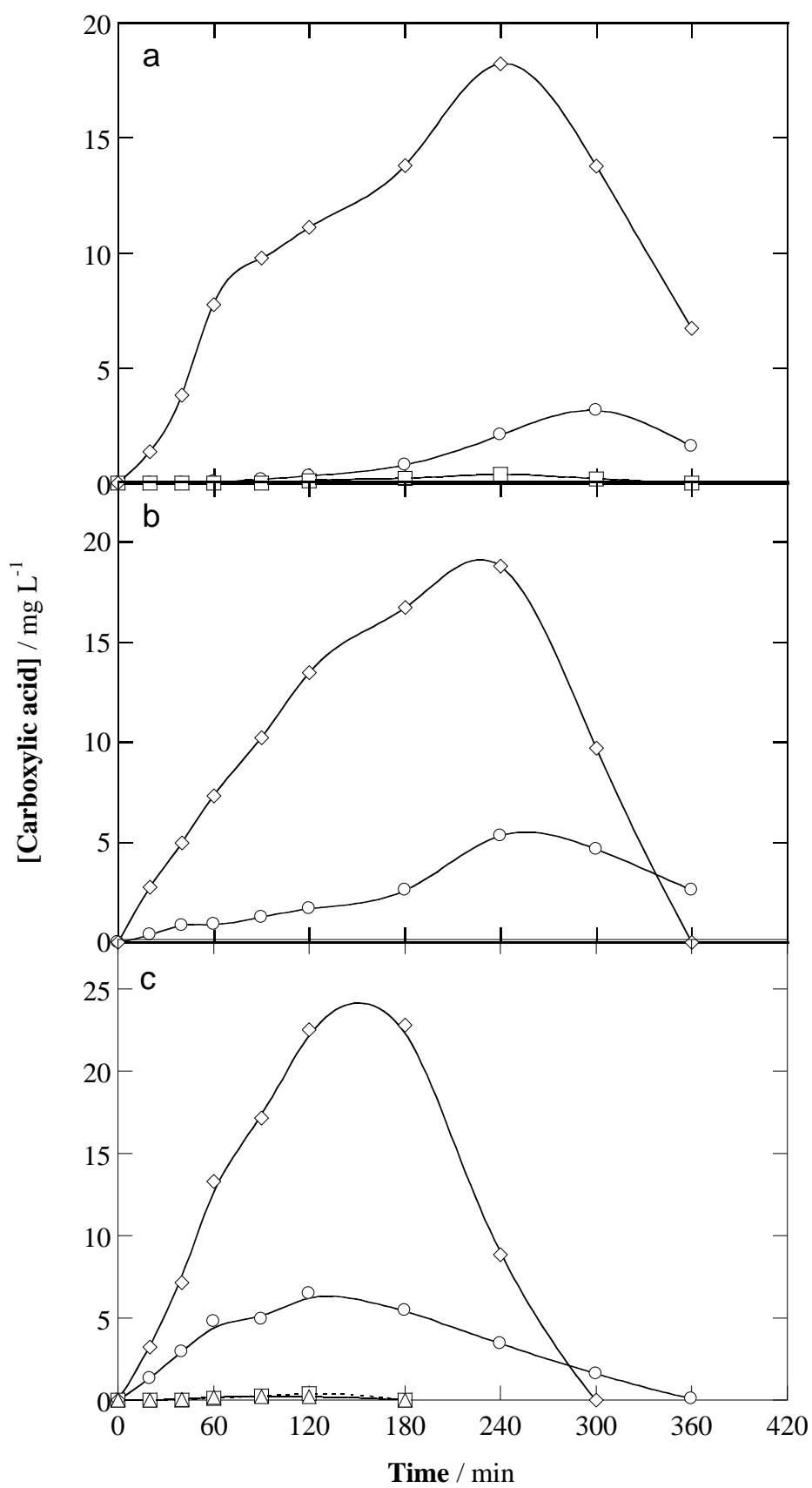


Fig. 6

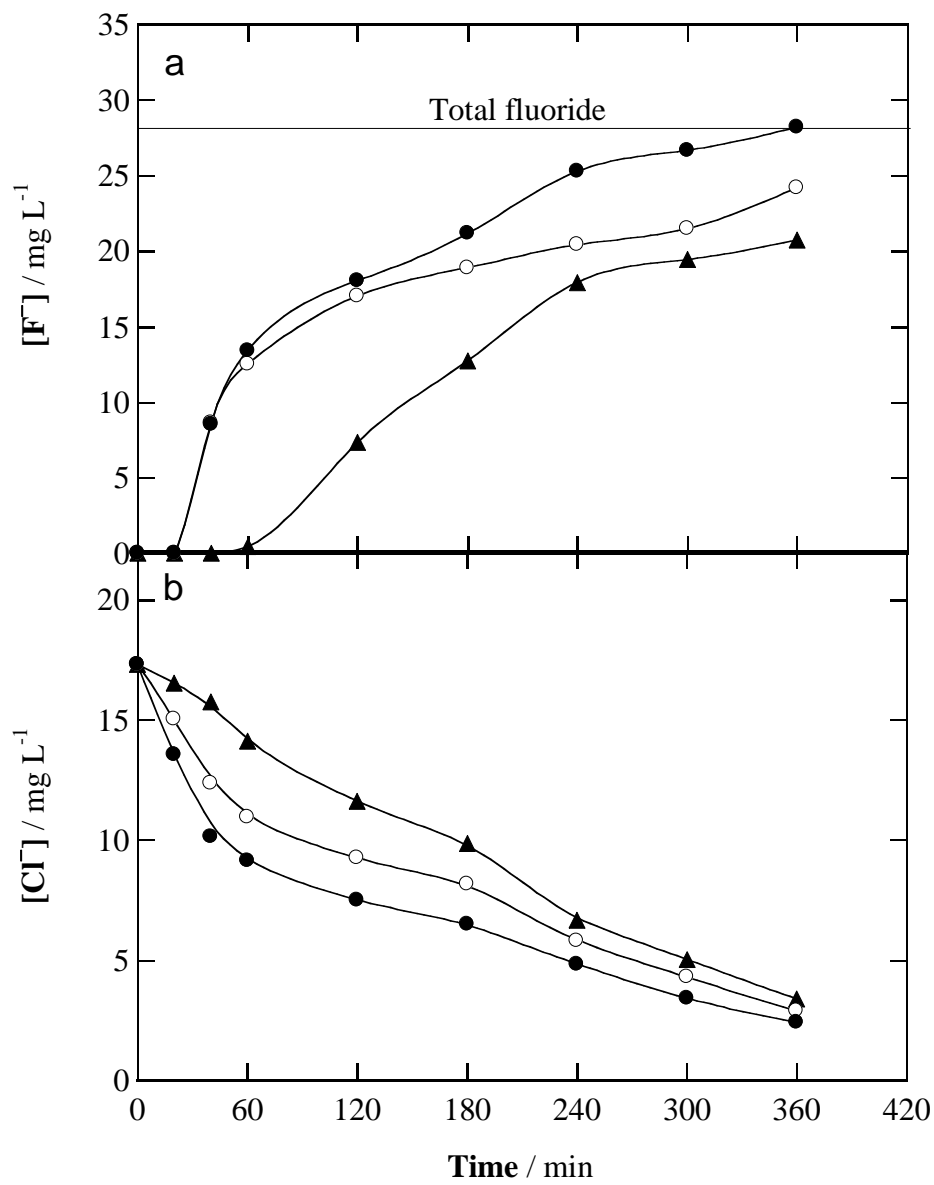


Fig. 7

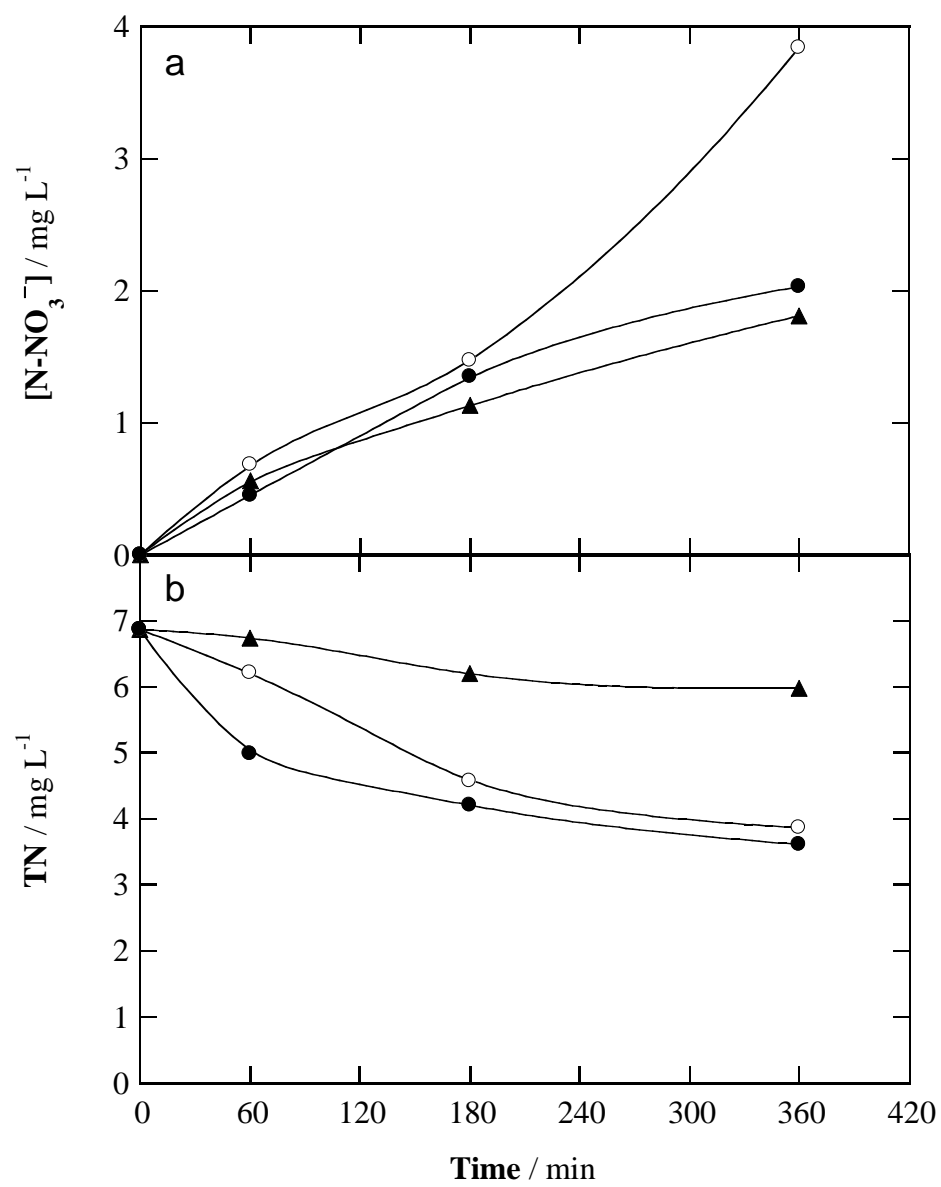


Fig. 8

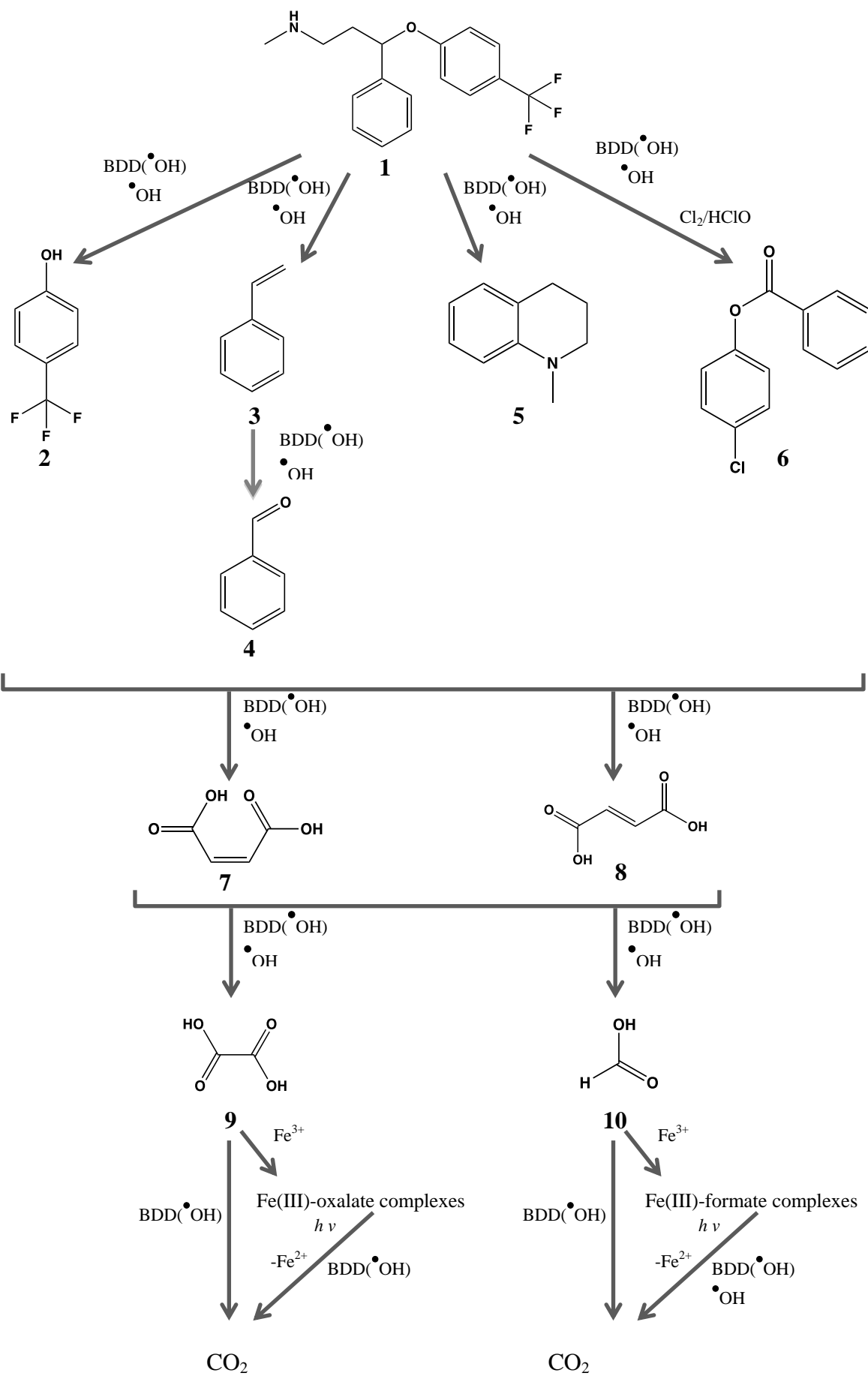


Fig. 9